The Role of the DNA-Binding Domains in CooA Activation†

Michael Kuchinskas,‡ Huiying Li,‡ Mary Conrad,§ Gary Roberts,§ and Thomas L. Poulos*,‡,||,⊥,#

Departments of Molecular Biology and Biochemistry, Physiology and Biophysics, and Chemistry and the Center in Chemical and Structural Biology, University of California—Irvine, Irvine, California 92697-3990, and Department of Bacteriology, University of Wisconsin—Madison, Madison, Wisconsin 53706

Received December 21, 2005; Revised Manuscript Received April 7, 2006

ABSTRACT: Carbon monoxide oxidation activator protein (CooA) is a dimeric carbon monoxide (CO) binding transcription factor that in the presence of CO promotes the transcription of genes involved in CO oxidation in *Rhodospirillum rubrum*. The off state (inactive) of Fe^{II} CooA has His and Pro as the two axial heme ligands. In contrast, in the on state, which is active in DNA binding, the Pro ligand bond has been replaced by CO. This occurs by the transient loss of the Pro ligand, thus generating a pentacoordinate heme that can bind CO. The active on state of CooA has two major structural differences from the off state, in addition to the displacement of the Pro ligand by CO. There is a repositioning of long C helices at the dimer interface and a concomitant reorientation of the hinge region between the DNA- and effector-binding domains within each monomer [Roberts et al. (2005) *J. Inorg. Biochem. 99*, 280−292]. To better understand the relationship of these conformational changes, we have removed the DNA-binding domains and compared CO binding to the truncated and full-length protein. The crystal structure of truncated Fe^{II} CooA is the same as that of the effector-binding domain of full-length Fe^{II} CooA, including the relative orientation of the homodimer and the ligation environment of the heme. Thus, removing the DNA-binding domains has little obvious effect on the structure of CooA in the inactive off state. However, CO binds about 2-fold more tightly and about 10 times more rapidly to truncated CooA. The rate of CO binding is known to be limited by the dissociation of the Pro heme ligand [Puranik et al. (2004) *J. Biol. Chem. 279*, 21096−21108]. Therefore, the absence of the DNA-binding domain makes it easier for the Pro ligand to dissociate from the heme iron, which also makes it easier for truncated CooA to adopt the on-state structure.

Carbon monoxide oxidation activator protein (CooA)[1] is a carbon monoxide (CO) sensing transcription factor from the photosynthetic bacterium *Rhodospirillum rubrum* that belongs to the catabolite activator protein (CAP) family of prokaryotic transcription factors (*1*). Similar to CAP, CooA is a homodimeric protein, with each monomer consisting of an effector-binding domain and a DNA-binding domain, which contains the classic helix−turn−helix DNA-binding motif. Although CAP and CooA share only 28% sequence identity, the DNA-binding helix−turn−helix motif exhibits an rms difference of only 1.3 Å, while the effector domain that binds cAMP in CAP and heme in CRP exhibits an rms difference of 1.6 Å. While cyclic AMP binds to the effector region in CAP, the effector domain in CooA binds heme, which, in turn, binds the effector molecule CO. The binding of CO to the heme promotes the binding of CooA to the 5′ promoter region of two operons, where CooA stimulates the transcription of genes responsible for CO oxidation (*2*). This enables *R. rubrum* to utilize CO as an energy source (*3*, *4*).

While there are structures of CAP both with (*5*) and without (*6*) DNA bound, all of these structures are in the DNA-binding on state with the effector, cAMP, bound. Our initial publication on the CooA structure (*7*) provided the first structure of a CAP-like transcription factor in the off state. Because CooA and CAP are structural homologues (Figure 1), the on state of CooA is expected to resemble the on state of CAP. Therefore, a comparison between the off-state CooA and on-state CAP structures provides insights on the range of motions induced by effector binding in each protein. Such a comparison shows that the DNA-binding domain undergoes a very large reorientation relative to the effector-binding domain upon activation. Although the two monomers of inactive CooA are in rather different orientations, they are both different from those of active CAP (Figure 1). Most importantly, the F helices, which make the critical sequence-specific DNA contacts, in both monomers of inactive CooA are not accessible for DNA binding. In the crystal structure of CooA, the C helix of monomer A is fully extended, having fused the C and D helices. In monomer B, these helices are separated by a break, termed the hinge region, as in active CAP, but the relative position of the two domains is completely different in CooA monomer B compared to active CAP. It is thus apparent that the DNA-

† This work was supported by NSF Grant MCB0315283 (to T.L.P.), NIH Grant GM 53228 (to G.R.), and the University of Wisconsin College of Agricultural and Life Sciences.

* To whom correspondences should be addressed. E-mail: poulos@uci.edu. Fax: 949-824-7020.

‡ Department of Molecular Biology and Biochemistry, University of California—Irvine.

§ Department of Bacteriology, University of Wisconsin—Madison.

|| Department of Physiology and Biophysics, University of California—Irvine.

⊥ Department of Chemistry, University of California—Irvine.

Center in Chemical and Structural Biology, University of California—Irvine.

[1] Abbreviations: CooA, carbon monoxide oxidation activator protein; CO, carbon monoxide; CAP, catabolite activator protein.

10.1021/bi052609o CCC: $33.50
Published on Web 05/20/2006

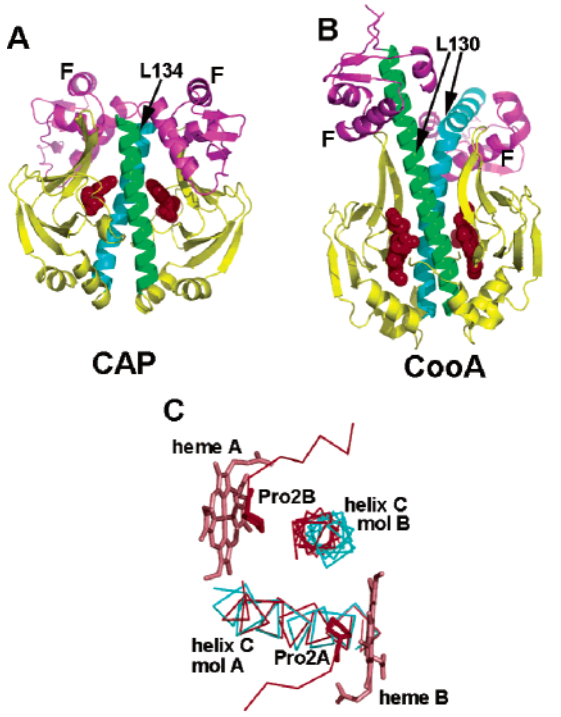

FIGURE 1: Structure of CAP and CooA. The cAMP and heme groups are highlighted as red space-filled models. The F helices that provide direct contact with DNA are labeled. (A) On-state structure of CAP with the effector, cAMP, bound. (B) Off-state structure of CooA in the reduced, CO-free form. Corresponding leucine residues 134 in CAP and 130 in CooA are in the region where the break in the C helices (highlighted in green and yellow) must occur to accommodate the activation of each protein. (C) Structural overlay of C-helical regions for CAP (blue) and CooA (red) in both monomers. The monomer A helices were superimposed, which illustrates that the off/on transition results in the motion of the monomer B helix relative to the monomer A helix. This motion causes steric crowding between the C helix of the monomer B helix and the Pro2 ligand, leading to the rupture of the Pro2−Fe bond.

binding domains can undergo rather large changes in orientation relative to the effector-binding domain.

In contrast to this view, using solution X-ray scattering, Akiyama et al. (*8*) suggest that the solution structure of CooA in the inactive CO-free off state is very similar to the CO-bound on state and that what we see in the off-state crystal structure with the C helix in one monomer completely extended and the other kinked is a consequence of crystal-packing forces. However, Akiyama et al. (*8*) calculate a fairly small difference in the radius of gyration, 25.9 Å, based on the crystal structure compared to an average value of 26.4 Å estimated from the experimental data, and what is not clear from scattering experiments is the relative population of various possible conformers. Moreover, crystal packing forces are weak and are not likely to force the protein to adopt a conformation that is not also accessible in solution. Thus, it is much more probable that the dimeric structure that we observe in the crystal structure is one of several conformers accessible in solution and is one of the many sampled in the scattering experiments. This leads to a picture of the off state as an ensemble of DNA-binding domain orientations, while the DNA-bound on state has only one orientation.

The key to understanding the CO-mediated allosteric transition from inactive to active forms of CooA is to explain

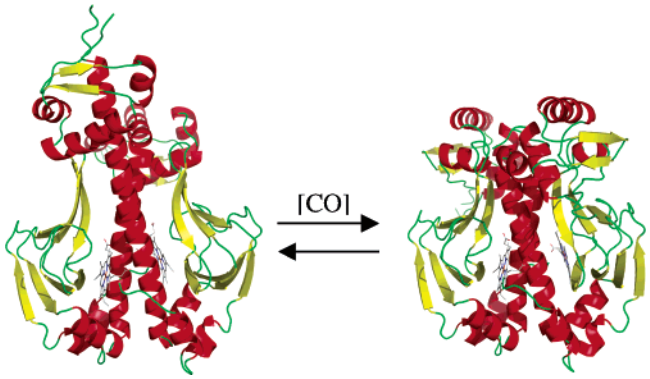

FIGURE 2: Off/on state equilibrium of CooA. On the left is the reduced structure of CooA (1FT9), and on the right is a hypothetical model for the on state of CooA, where the DNA-binding domains have made their transition to bind DNA. Binding of CO to the heme shifts the equilibrium toward the on state.

how CO binding, at the heme iron, can lead to reorientation in the C-helix hinge region some 25 Å away. A careful comparison between on-state CAP and off-state CooA indicated that there is a change at the dimer interface and especially at the interface between the C helices (*7*). That is, if the C helices of one monomer of CAP and CooA are superimposed, the C helices in the other monomers of each protein do not superimpose (Figure 1). From this simple change, a relatively detailed picture of the CooA activation process has been developed (*7*, *9*). This repositioning of the C helices transmits a signal from the heme region to the hinge region, which in turn stabilizes either the active or inactive positions of the DNA-binding domains. However, the C-helix repositioning is incompatible with the retention of the Pro2−Fe bond. The transient deligation of the Pro2 ligand therefore results in a pentacoordinate heme that can now bind CO. On the basis of the Monod−Wyman−Changeux model for allosteric transitions (*10*), CooA is viewed as an equilibrium mix of the on- and off-state structures, with the off state favored in the absence of CO (Figure 2).

The very close similarity in the structure of the DNA-binding domains of CooA and CAP indicates that these domains themselves are minimally changed upon activation. Instead, the allosteric transition affects only the orientation of the DNA-binding domains relative to that of the effector-binding domain. Studying the structural and functional properties of the effector-binding domain in the absence of the DNA-binding domain provides a way of testing the impact of the DNA-binding domain reorientation on the energetics of CO binding. In this study, we describe the structure and CO-binding properties of a truncated version of CooA lacking the DNA-binding domain.

MATERIALS AND METHODS

Protein Expression and Purification. Full-length (wild-type) CooA was expressed and purified as previously described (*11*), with slight modifications as follows. Cells were grown in 2xYT media and lysed through two passes in a microfluidics ML-100 cell homogenizer at 18 000 psi. The resuspended ammonium sulfate pellet was loaded directly onto a Superdex S200 preparative column (Pharmacia). The best fractions were then loaded onto a Q-sepharose fast-flow column (Pharmacia). The final combined fractions were estimated to be >95% pure via sodium

Table 1: Data Collection and Refinement Statistics

data set	CooA heme domain
PDB code	1FT9
cell dimensions (Å)	$a = 71.23$
(SG: $P4_1$)	$b = 71.23$
	$c = 143.73$
data resolution (Å)	2.70
total observations	184 353
unique reflections	19 766
R_{sym}[a]	0.066 (0.650)[b]
$\langle I/\sigma \rangle$	22.3 (2.0)[b]
completeness (%)	99.8 (99.9)[b]
reflection used in refinement	18 584
R factor[c]	0.2079
R_{free}[d]	0.2640
number protein atoms	4148
number heterogen atoms	172
number water molecules	63
rms deviation	
bond length (Å)	0.007
bond angle (deg)	1.3

[a] $R_{sym} = \sum|I - \langle I \rangle|/\sum I$, where I is the observed intensity of a reflection and $\langle I \rangle$ is the averaged intensity of multiple observations of the reflection and its symmetry mates. [b] The values in parentheses were obtained in the outermost resolution shell. [c] R factor $= \sum||F_o| - |F_c||/\sum|F_o|$, where F_o and F_c are the observed and calculated structure factors, respectively. [d] R_{free} was calculated with the 5% of reflections set aside randomly throughout the refinement.

dodecyl sulfate−polyacrylamide gel electrophoresis (SDS−PAGE).

Escherichia coli strain UQ1904, expressing the heme domain containing N-terminal amino acids through methionine 131 plus six additional histidine residues, was constructed by using appropriate oligo primers to modify the cloned wild-type *cooA* sequence. The heme domain was expressed, and the cells were lysed as with the full-length CooA and purified via nickel−nitrilotriacetic acid (Ni−NTA) agarose (Qiagen). Protein fractions with purity >95% were precipitated with ammonium sulfate and resuspended in 25 mM 3-(*N*-morpholino)propanesulfonic acid (MOPS) at pH 7.4, 500 mM NaCl, and 2 mM dithiothreitol (DTT). The protein solution was subsequently desalted using the same buffer to remove any trace amounts of ammonium sulfate and imidazole.

Determination of Equilibrium Binding Constants. All protein samples and buffers were made anaerobic by exchange with O_2-free argon on a vacuum manifold. Anaerobic handling was performed in a soft-sided glovebox (Coy Laboratories). CO binding to both full-length and truncated forms of CooA was monitored by measuring spectral changes at 558 nm using a Varian Cary 3E UV−vis spectrophotometer in 1.5 mL sealed anaerobic cuvettes (Starna Cells). Protein samples (2 μM by heme) were reduced with dithionite (5 mM) and titrated with a saturated solution of O_2-free CO (1 mM). Headspace was limited to the volume of total CO added (<1% of total volume) to minimize degassing of CO. Data were fitted as previously described (*12*).

Determination of CO Association Rate Constants. Rates of CO binding were measured using an Applied Photophysics Ltd. SX.18MV-R stopped-flow instrument, and absorbance changes were measured at 558 nm. Protein samples (20 μM) were reduced with dithionite and combined with various

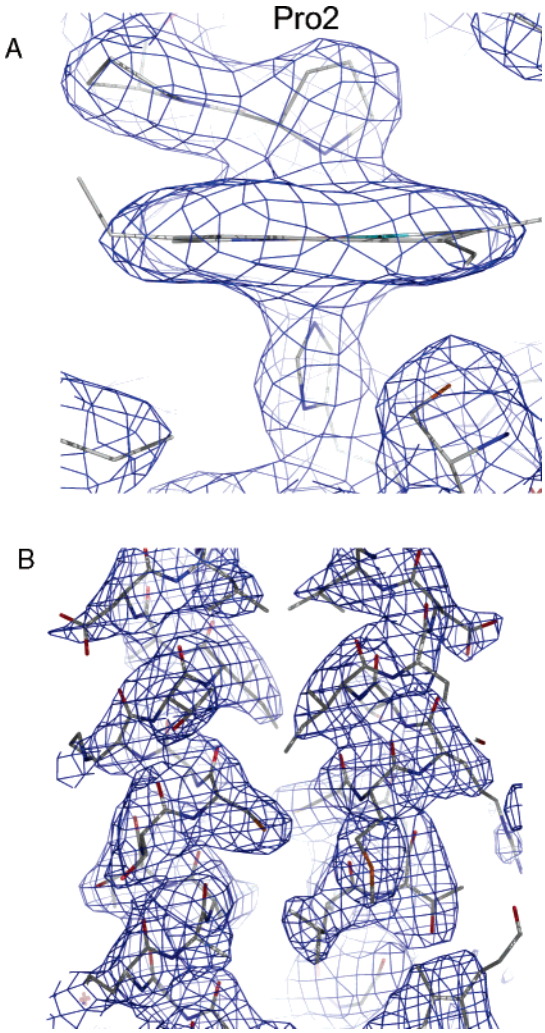

FIGURE 3: $2F_o - F_c$ composite omit electron-density maps contoured at 1.0σ for (A) the heme environment and (B) the interface between the C helices.

concentrations of O_2-free CO. To obtain data at higher CO concentrations, asymmetric mixing experiments were performed using a 2:1 ratio of CO/protein.

Crystallization and Data Collection. Crystals were grown under anaerobic conditions at 22 °C by the hanging-drop, vapor diffusion method in Nextal plates. All solutions were made anaerobic by continuous exchange with O_2-free argon on a vacuum manifold. The reservoir solution consisted of 20% (w/v) poly(ethylene glycol) (PEG) 8000, 100 mM 2-(cyclohexylamino)ethylsulfonic acid (CHES) at pH 9.0, and 5 mM dithionite. Drops consisted of 2 μL of reduced truncated CooA (12 mg/mL) and 2 μL of reservoir solution. Large (~100 × 500 μm) rod-shaped crystals formed after 3 weeks but diffracted weakly. Dehydration of the crystals was performed via the addition of 1 μL of dehydration solution [30% (w/v) PEG 8000, 20% glycerol, 100 mM CHES at pH 9.0, and 5 mM dithionite] to the 4 μL drop. The drop was then moved to a new well and allowed to equilibrate over the dehydrating solution for 1 week. This process improved the resolution of the data from ~6 to 2.7 Å. Crystals were found to belong to the tetragonal space group $P4_1$ with unit-cell dimensions of $a = 71.23$, $b = 71.23$, and $c = 143.73$ Å. X-ray intensity data were collected at the Stanford Synchrotron Radiation Laboratory on beamline 9-1. Data

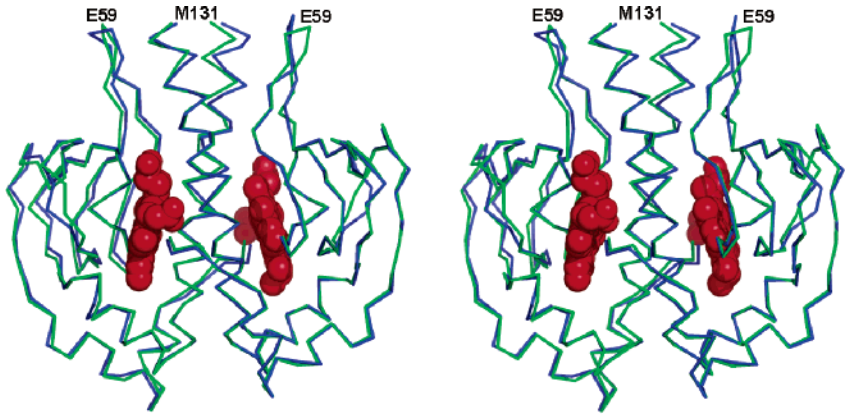

FIGURE 4: Stereodiagram showing the superimposition of truncated CooA (green) and full-length CooA (blue). Mol A and B refer to molecules A and B in the dimer.

were indexed, integrated, and scaled using Denzo and Scalepack (*13*).

Molecular replacement using MolRep (*14*) was performed using the heme domain of the wild-type protein as a search model. The correct solution was found to contain four subunits (two dimers) per asymmetric unit. The structure was refined using CNS (*15*). Final data parameters are summarized in Table 1.

RESULTS

Crystal Structure. The crystallographic structure of the Fe^{II} form of the heme domain was determined to a resolution of 2.7 Å. Electron-density maps of the C-helix interface and heme-ligation environment are shown in Figure 3. Figure 4 shows a comparison between truncated and full-length CooA. The overall root-mean-square (rms) deviation for 130 common Cα atoms is 0.7 Å. The only significant deviation is near the C-terminal Met131. The surface β turn centered on Glu59 shifts about 5 Å. The DNA-binding domain contacts Glu59 in full-length CooA; therefore, it is not surprising that the removal of the DNA-binding domain results in the movement of Glu59. However, the core of the effector domain remains unchanged, including the dimer interface and the relative positioning of the two C helices. The heme-ligation environment consisting of His77 and Pro2 as axial heme ligands also remains unchanged.

Equilibrium Titration. CO titration curves for both full-length and truncated CooA are shown in Figure 5. For full-length CooA, the apparent $K_D = 0.65\ \mu M$, which is similar to the $K_D = 2.0\ \mu M$ published previously (*12*). The truncated protein exhibited an apparent $K_D = 0.32\ \mu M$. These experiments were performed multiple times (~20), and in each experiment, the apparent K_D value for the heme domain was always lower than in full-length CooA, indicating that removal of the DNA-binding domain increases the affinity for CO.

Stopped-Flow Studies. The association rates of full-length and truncated CooA are shown in Figure 6. The binding of CO is slow, biphasic, and exhibits a hyperbolic dependence on the CO concentration (Figure 6). The kinetics of CO binding has previously been analyzed in detail, and the dissociation of the Pro2 heme ligand was shown to be rate-limiting (*12*). Therefore, the maximum k_{obs} measured in the stopped-flow studies is directly related to the rate of Pro ligand dissociation. For full-length CooA, we obtain values

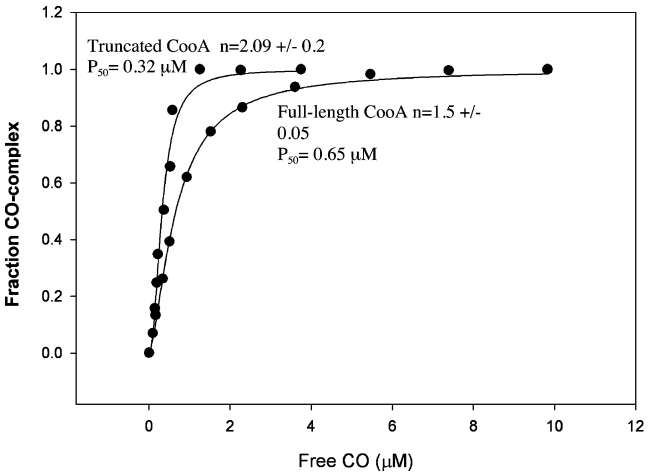

FIGURE 5: Titration curves for the binding of CO to truncated and full-length CooA. Lines represent the best fit to the Hill equation.

of 0.4 and 0.2 s^{-1} for the fast and slow phases, respectively. Truncated CooA also exhibits biphasic binding kinetics, except the rates increase about 10-fold to 4.0 and 1.0 s^{-1}. This indicates that, in the absence of the DNA-binding domain, Pro2 dissociates from the heme iron faster than in full-length CooA.

DISCUSSION

Unraveling the structural basis for the CO-induced allosteric switch in CooA will require the structure of the CooA−CO complex and possibly the CooA−CO complex bound to DNA. Until then, the simplest working hypothesis is to assume a simple allosteric two-state model, where the on and off states of CooA are in equilibrium. While the on state is very likely dominated by a single conformer, the same is not true for the off state. As the structure of full-length off-state CooA shows, only monomer A is totally extended, while monomer B has a bend in the hinge region between the DNA-binding and effector-binding domains. Because it is sterically impossible for both monomers to simultaneously adopt the completely extended form of monomer A, it is very likely that in solution the orientations of the DNA-binding domains are not fixed. In contrast, the requirements of proper F-helix positioning for specific DNA interactions argue that the on state of CooA is stabilized by inter- and intramolecular contacts. This reorientation of the DNA-binding domains is stabilized by the repositioned C helices,

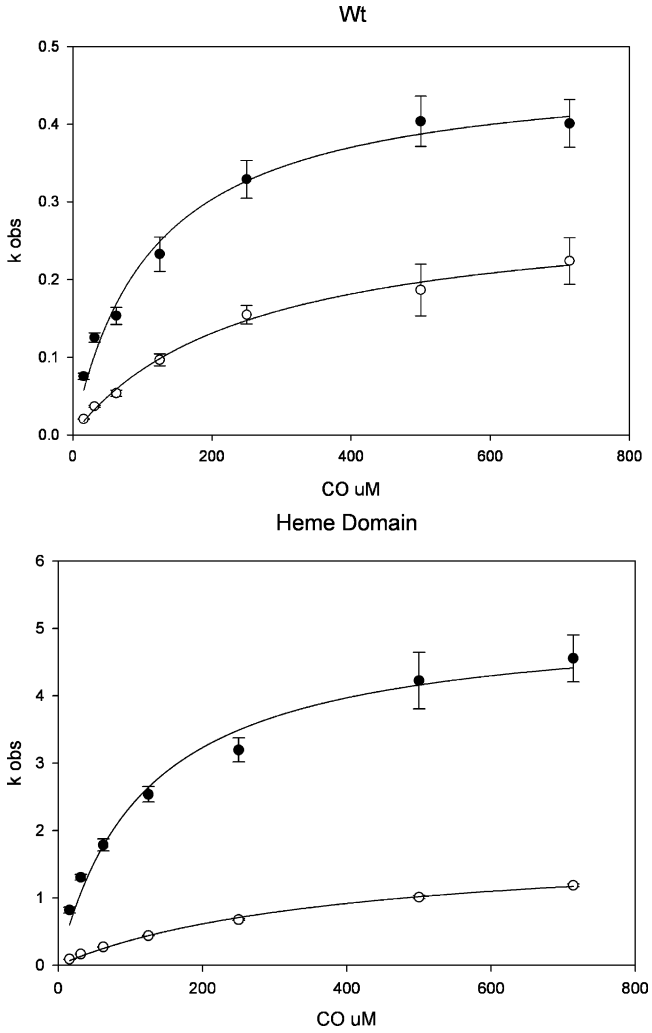

FIGURE 6: Kinetics of CO binding. Plot of pseudo-first-order rate constants versus the CO concentration for the full-length (top) and truncated (bottom) CooA. The slow phase of the reaction is indicated by ○, and the fast phase is indicated by ●.

which in turn requires the breakage of the Pro2−Fe bond. CO binding stabilizes this Pro2−Fe bond displacement and thus shifts the on/off equilibrium in favor of the on state.

Our results show that removal of the DNA-binding domain has no effect on the heme-binding effector domain structure of CooA, except for changes near Glu59, which contacts the DNA-binding domain in full-length CooA. However, truncated CooA binds CO more tightly and more rapidly than does full-length CooA. Even so, the kinetics of CO binding remains biphasic as in full-length CooA. Such biphasic kinetics has been attributed to the cooperative CO binding, such that the binding of the first CO to heme A slows down the dissociation of the Pro2 from heme B (*12*). Truncated CooA behaves similarly with respect to biphasic kinetics, but the binding of CO is faster. Because CO binding is limited by dissociation of the Pro2 ligand (*12*), the removal of the DNA-binding domain makes it easier for the Pro2 ligand to dissociate. One possible explanation is that without the DNA-binding domain fewer inter- and intrasubunit contacts must be broken in going from the off to on state, which lowers the activation energy barrier for rupture of the Pro2−Fe bond. For example, without the DNA-binding domain, the hinge reorientation at Leu130, which necessitates breaking helical hydrogen bonds, is no longer required. Removal of this energetic barrier thus lowers the activation energy barrier in the on/off transition, which is reflected in a faster dissociation of the Pro2 ligand and, hence, more rapid CO binding. A more specific example is an ion pair that must be broken in the off/on transition. In inactive CooA, Glu59 of monomer A forms an ion pair/hydrogen bond with Arg138 in monomer B, but in active CAP, the analogous Arg residue (Arg142) is positioned to hydrogen bond with a purine carbonyl oxygen atom about 3 Å away. Thus, the Glu59−Arg138 salt bridge is most likely to be broken in the off state, and the energy lost is regained when Arg138 forms new interactions with the DNA. Without the DNA-binding domain, Arg138 is missing and, thus, there is no need to break an off-state ion pair, which again lowers the activation energy in the on/off transition.

These differences can be more quantitatively analyzed by assuming a simple relationship between rates of CO binding and activation energy, which enables estimates to be made on the activation energy for disruption of the Pro2−Fe bond. The rate of CO binding to the pentacoordinate heme in CooA estimated from flash photolysis studies is about 30 000 s^{-1} (*12*, *16*). Our stopped-flow experiments, where Pro2 dissociation is limiting, give 0.4 s^{-1} for the fast phase of the reaction in full-length CooA. This 75 000-fold difference in rate is due to the barrier imposed by dissociation of the Pro2 ligand. If we assume simple transition-state theory and $k \propto \exp(\Delta G^*/RT)$, where ΔG^* = the activation energy and k = the rate of CO binding, then the activation energy barrier for Pro2 dissociation is on the order of 6.7 kcal/mol. By a similar analysis, an increase in the rate of CO binding by 10-fold owing to the removal of the DNA-binding domains translates into a lowering of the activation energy barrier for Pro2 dissociation by 1.4 kcal/mol. This suggests that the intra- and intermolecular on/off changes involving the DNA-binding domains contribute a modest 1−2 kcal/mol in Pro2 dissociation. Therefore, most of the "work" in the allosteric transition is due to changes in the effector domain as discussed by Puranik et al. (*12*). The switch to the on state when Pro dissociates and the heme binds CO unmasks new interactions that lock the DNA domains into the orientation favorable for DNA binding. Similar arguments can explain why truncated CooA binds CO with a higher affinity than full-length CooA. In the simple two-state on/off model, the tighter binding indicates that the K_{eq} between the on/off states has shifted toward the on state in truncated CooA. There also is higher cooperativity in truncated CooA as evidenced by an increase in the Hill coefficient for CO binding from ≈1.5 in full-length CooA to ≈2.0 in truncated CooA.

In summary, our results show that the DNA-binding domains play no role in the structure of the off-state heme-binding domain. The DNA-binding domains do contribute about a factor of 10 in the rate of Pro2 dissociation from the heme iron, although in terms of the activation energy of Pro2−Fe dissociation, this factor of 10 is a rather modest, 1−2 kcal/mol. This means that a majority of the energetic changes that occur in the off/on transition are centered in the effector heme-binding domain. Given the very close structural homology between CooA, CAP, and related transcription factors, it is very likely that the DNA-binding domains also play a minor role in the allosteric transition in other members of the CAP family of transcription factors.

ACKNOWLEDGMENT

The authors thank Bob Kerby and Hwan Youn for valuable discussions and critical reading of the manuscript.

REFERENCES

1. Shelver, D., Kerby, R. L., He, Y., and Roberts, G. P. (1995) Carbon monoxide-induced activation of gene expression in *Rhodospirillum rubrum* requires the product of cooA, a member of the cyclic AMP receptor protein family of transcriptional regulators, *J. Bacteriol. 177*, 2157−2163.
2. He, Y., Shelver, D., Kerby, R. L., and Roberts, G. P. (1996) Characterization of a CO-responsive transcriptional activator from *Rhodospirillum rubrum*, *J. Biol. Chem. 271*, 120−123.
3. Kerby, R. L., Ludden, P. W., and Roberts, G. P. (1995) Carbon monoxide-dependent growth of *Rhodospirillum rubrum*, *J. Bacteriol. 177*, 2241−2244.
4. Ensign, S. A., Bonam, D., and Ludden, P. W. (1989) Nickel is required for the transfer of electrons from carbon monoxide to the iron−sulfur center(s) of carbon monoxide dehydrogenase from *Rhodospirillum rubrum*, *Biochemistry 28*, 4968−4973.
5. Schultz, S. C., Shields, G. C., and Steitz, T. A. (1991) Crystal structure of a CAP−DNA complex: The DNA is bent by 90°, *Science 253*, 1001−1007.
6. Passner, J. M., Schultz, S. C., and Steitz, T. A. (2000) Modeling the cAMP-induced allosteric transition using the crystal structure of CAP-cAMP at 2.1 Å resolution, *J. Mol. Biol. 304*, 847−859.
7. Lanzilotta, W. N., Schuller, D. J., Thorsteinsson, M. V., Kerby, R. L., Roberts, G. P., and Poulos, T. L. (2000) Structure of the CO sensing transcription activator CooA, *Nat. Struct. Biol. 7*, 876−880.
8. Akiyama, S., Fujisawa, T., Ishimori, K., Morishima, I., and Aono, S. (2004) Activation mechanisms of transcriptional regulator CooA revealed by small-angle X-ray scattering, *J. Mol. Biol. 341*, 651−668.
9. Kerby, R. L., Youn, H., Thorsteinsson, M. V., and Roberts, G. P. (2003) Repositioning about the dimer interface of the transcription regulator CooA: A major signal transduction pathway between the effector and DNA-binding domains, *J. Mol. Biol. 325*, 809−823.
10. Monod, J., Wyman, J., and Changeux, J. P. (1965) On the nature of allosteric transitions: A plausible model, *J. Mol. Biol. 12*, 88−118.
11. Shelver, D., Thorsteinsson, M. V., Kerby, R. L., Chung, S. Y., Roberts, G. P., Reynolds, M. F., Parks, R. B., and Burstyn, J. N. (1999) Identification of two important heme site residues (cysteine 75 and histidine 77) in CooA, the CO-sensing transcription factor of *Rhodospirillum rubrum*, *Biochemistry 38*, 2669−2678.
12. Puranik, M., Nielsen, S. B., Youn, H., Hvitved, A. N., Bourassa, J. L., Case, M. A., Tengroth, C., Balakrishnan, G., Thorsteinsson, M. V., Groves, J. T., McLendon, G. L., Roberts, G. P., Olson, J. S., and Spiro, T. G. (2004) Dynamics of carbon monoxide binding to CooA, *J. Biol. Chem. 279*, 21096−21108.
13. Otwinowski, Z., and Minor, W. (1997) Processing of X-ray diffraction data collected in oscillation mode, *Methods Enzymol. 276*, 307−326.
14. Vagin, A., and Teplyakov, A. (2000) An approach to multi-copy search in molecular replacement, *Acta Crystallogr., Sect. D: Biol. Crystallogr. 56* (part 12), 1622−1624.
15. Brunger, A. T., Adams, P. D., Clore, G. M., DeLano, W. L., Gros, P., Grosse-Kunstleve, R. W., Jiang, J. S., Kuszewski, J., Nilges, M., Pannu, N. S., Read, R. J., Rice, L. M., Simonson, T., and Warren, G. L. (1998) Crystallography and NMR system: A new software suite for macromolecular structure determination, *Acta Crystallogr., Sect. D: Biol. Crystallogr. 54* (part 5), 905−921.
16. Uchida, T., Ishikawa, H., Takahashi, S., Ishimori, K., Morishima, I., Ohkubo, K., Nakajima, H., and Aono, S. (1998) Heme environmental structure of CooA is modulated by the target DNA binding. Evidence from resonance Raman spectroscopy and CO rebinding kinetics, *J. Biol. Chem. 273*, 19988−19992.

BI052609O